Int. J. Electrochem. Sci., 8 **(2013)** 520 - 534

International Journal of
ELECTROCHEMICAL
SCIENCE
www.electrochemsci.org

Fabrication of Highly Sensitive Phenyl Hydrazine Chemical Sensor based on as-grown ZnO-Fe_2O_3 Microwires

Mohammed M. Rahman[1,2,*], *George Gruner*[1, 3], *Mohammed Saad Al-Ghamdi*[4], *Muhammed A. Daous*[5] , *Sher Bahadar Khan*[1,2], *Abdullah M. Asiri*[1,2]

[1]Center of Excellence for Advanced Materials Research, King Abdulaziz University, Jeddah 21589, P.O. Box 80203, Saudi Arabia
[2]Chemistry Department, Faculty of Science, King Abdulaziz University, P.O. Box 80203, Jeddah 21589, Saudi Arabia
[3]Department of Physics, University of California Los Angeles, USA.
[4]Physics Department, Faculty of Science, King Abdulaziz University, P.O. Box 80203, Jeddah 21589, Saudi Arabia
[5]Chemical Engineering, Faculty of Engendering, King Abdulaziz University, Jeddah 21589, Saudi Arabia
[*]E-mail: mmrahman@kau.edu.sa

Received: 26 August 2012 / *Accepted:* 27 November 2012 / *Published:* 1 January 2013

As-grown ZnO-Fe_2O_3 microwires were prepared by a wet-chemical process using reducing agents in alkaline medium and characterized by UV/vis., FT-IR, Raman, electron-dispersive (EDS) spectroscopy, powder X-ray diffraction (XRD), and field-emission scanning electron microscopy (FESEM). They were deposited on a gold electrode (AuE, surface area, 0.0216 cm^2) to fabricate a chemi-sensor with a fast response towards toxic phenyl hydrazine (PhHyd) chemical in phosphate buffer solution (PBS). The chemi-sensor was also exhibited higher sensitivity and long-term stability, and enhanced electrochemical response towards toxic PhHyd. The calibration plot was linear (r^2 = 0.9389) over the 1.0 nM to 10.0 mM PhHyd concentration ranges. The sensitivity and detection limit were calculated about 8.33 $\mu Acm^{-2}mM^{-1}$ and 0.67 ± 0.05 nM (signal-to-noise ratio, at a SNR of 3) respectively. Here the possible future prospective uses of the ZnO-Fe_2O_3 microwires in terms of chemical sensing are discussed.

Keywords: ZnO-Fe_2O_3 micro-wire; Wet-chemical method; Phenyl hydrazine; I-V technique; Sensitivity

1. INTRODUCTION

Semiconductor doped materials have attracted much attention because of their unique properties and potential applications in all areas of disciplines [1-12]. The simplest synthetic way to

doped-materials is possibly self-aggregation, in which ordered aggregate materials are prepared in economical approaches [13]. Though, it is still a big-challenge to develop simple and reliable route for microstructures metal oxide with designed chemical components and controlled morphologies, which strongly influence the properties of semiconductor materials [14]. The significance of safety for human-beings as well as environments has been considered with great attention in doped semiconductor sensors for toxic chemical detection by reliable methods [15]. Semiconductor micro-structure materials are very sensitive owing to their smaller particle size and higher active surface-area as compared to the transition materials in micro-meter range. Microstructures have also displayed a huge-attention due to their promising properties occurring of large active surface area, high stability, quantum confinement, and high-porosity, and permeability (meso-porous nature), which are contingent on the shape and size of the microcrystal [16]. During the last two decades, semiconductor materials have also received significant attention due to their electronic, magnetic, electrical, optoelectronic, mechanical properties, and their prospective applications in nanotechnology fields. Doped materials might be a promising candidate because of their high specific surface-area, low-resistance, fascinating electrochemical, and optical properties [17,18]. Zinc-ferrites are technologically significant doped materials due to their exceptional mechanical, electrical, thermal, and magnetic characteristics. Recently, it has gained much attention in transition metal doped-semiconductors in order to develop their chemical properties and improve their potential applications [19-28]. It has not only studied the fundamental of magnetism, but also has enormous potential in technological aspects (ie, magnetic materials, sensors, catalysts, and absorbent materials) [29-31]. Till to date, several articles are reported on the basis of doped materials preparation and studied the magnetic properties [32,33]. The ZnO-Fe_2O_3 micro-wire was prepared using simple, facile, economical, one-step, reproducible and reliable low-temperature wet-chemical process. The structure and morphology of the as-grown microwires were investigated and applied for the development of highly sensitive chemical sensor. Hence, chemical sensing investigations have been explored with the metal oxide for the detection and quantification of various chemicals such as methanol, ethanol, chloroform, dichloromethane, and acetone, etc, which are not environmental safe [34]. The chemical sensing mechanism with metal oxides thin-films is utilized mainly the properties of porous-film formed by physi-sorption and chemi-sorption techniques. The toxic chemical detection is based on the current responses of the fabricated thin-film, which caused by the presence of chemical component in reaction system in aqueous phase [35-37]. The key-attempts are focused on quantifying the minimum amount of PhHyd necessary for the fabricated ZnO-Fe_2O_3 microwires sensors for electrochemical approaches.

Here, a wet-chemical process is used to assemble as-prepared ZnO-Fe_2O_3 with practically controlled microwires-shape structure, which is exposed a control-morphological development in microstructure materials and efficient applications. With most of the significant involvement displayed on un-doped material, there have been more and more attention focused to explore the doped counterparts. For semiconductor materials, doping is an excellent application to enhance the optical and electrical properties, which improves the development of frequent electronic and optoelectronic miro-devices. ZnO-Fe_2O_3 microwires allow very sensitive transduction of the liquid/surface interactions to modify in the chemical possessions. ZnO-Fe_2O_3 microwire sensors are fabricated by a simple process on a side-polished AuE surface and measured the chemical sensing performance

considering PhHyd at room conditions. To best of our knowledge, this is the first report for detection of toxic PhHyd with as-grown ZnO-Fe_2O_3 microwires using simple and reliable I-V method in short response time.

2. EXPERIMENTAL SECTIONS

2.1. Materials and Methods

Ferric chloride, zinc chloride, butyl carbitol acetate, ethyl acetate, *urea*, ammonia solution (25%), and all other chemicals were in analytical grade and purchased from Sigma-Aldrich Company. FT-IR spectra were investigated on a spectrum-100 FT-IR spectrophotometer in the mid-IR range purchased from Bruker (ALPHA, USA). The powder X-ray diffraction (XRD) patterns were recorded by X-ray diffractometer from PANalytical diffractometer equipped with Cu-$K_{\alpha 1}$ radiation (λ =1.5406 nm) using a generator voltage of 45.0 kV and a generator current of 40.0 mA were applied for the determination. Morphology, size, and structure of as-grown ZnO-Fe_2O_3 micro-wire were recorded on FE-SEM instrument from JEOL (JSM-7600F, Japan). Raman spectrometer was used to measure the Raman shift of as-grown ZnO-Fe_2O_3 microwires using radiation source (Ar^+ laser line, λ; 513.4 nm), which was purchased from Perkin Elmer (Raman station 400, Perkin Elmer, Germany). Elemental analysis was investigated using oxford-EDS system from JEOL (JSM-7600F, Japan). The λ_{max} (302.0 nm) of as-grown ZnO-Fe_2O_3 microwire was executed using UV/visible spectroscopy Lamda-950, Perkin Elmer, Germany. I-V technique (two electrodes system) is employed by Kethley-Electrometer from USA.

2.2. Preparation and growth mechanism of as-grown ZnO-Fe_2O_3 microwires

Large-scale synthesis of ZnO-Fe_2O_3 microwire was prepared by wet-chemical process at low-temperature using zinc chloride ($ZnCl_2$), iron chloride ($FeCl_3$), and ammonium hydroxide (NH_4OH). In a typical reaction process, 0.1 M $ZnCl_2$ dissolved in 50.0 ml deionized (DI) water mixed with 50.0 ml DI solution of 0.1 M $FeCl_3$ and 50.0 ml of 0.1 M urea under continuous stirring. The pH of the solution was adjusted to 8.1 by the addition of NH_4OH and resulting mixture was shacked and stirred continuously for 20.0 minutes at room conditions. After stirring, the mixture was then put into conical flux and heat-up at 160.0 ^oC for 8.0 hours. The temperature of the solution mixture was controlled manually throughout the reaction process at 92.0 ^oC. After heating the reactant mixtures, the flux was kept for cooling at room conditions until it reached to room temperature. The final products were achieved, which was washed with DI water, ethanol, and acetone for several times subsequently and dried at room-temperature for structural and optical characterizations. The growth mechanism of ZnO-Fe_2O_3 microwire can be apprehended on the basis of chemical reactions and nucleation, as well as growth of ZnO-Fe_2O_3 crystals. The probable reaction mechanisms are proposed for achieving the doped metal oxides, which are suggested in below.

$$ZnCl_2(s) \rightarrow Zn^{2+}_{(aq)} + 2Cl^-_{(aq)} \quad \text{(i)}$$

$$FeCl_3(s) \rightarrow Fe^{3+}_{(aq)} + 3Cl^-_{(aq)} \quad \text{(ii)}$$

$$NH_4OH_{(aq)} \rightarrow NH_4^+{}_{(aq)} + OH^-{}_{(aq)} \quad \text{(iii)}$$

$$Fe^{3+}{}_{(aq)} + Zn^{2+}{}_{(aq)} + 8OH^-{}_{(aq)} \rightarrow ZnO.Fe_2O_{3(s)} + 4H_2O \quad \text{(iv)}$$

The precursors of $ZnCl_2$ and $FeCl_3$ are soluble in alkaline medium (NH_4OH reagent) according to the equation of (i) - (ii). After addition urea (as surfactant) with NH_4OH into the mixture of metal chlorides solution, it was strongly stirred for few minutes at room temperature. The reaction is enhanced gradually according to the equations (iii) to (iv). Then the solution was washed thoroughly with acetone and kept for drying at room temperature. During the total synthesis process, urea and NH_4OH acts a pH buffer to control the pH value of the solution and slow donate of OH^- ions. When the concentrations of the Zn^{2+}, Fe^{3+}, and OH^- ions are reached above the critical value, the precipitation of ZnO-Fe_2O_3 (Fe_2O_3 codoped ZnO) nuclei is initiated. As there is high concentration of Zn^{2+} ion in the solution, the nucleation of ZnO-Fe_2O_3 crystals become easier due to the lower activation energy barrier of heterogeneous nucleation. However, as the concentration of Fe^{3+} subsistence, a number of larger ZnO-Fe_2O_3 crystals with a rod-shape morphology form in micro-level. The shape of as-grown ZnO-Fe_2O_3 microwire is approximately reliable with the growth pattern of crystals [38]. Finally, as-prepared doped products were characterized in detail in terms of their morphological, structural, optical properties, and applied for PhHyd chemical sensors.

2.3. Fabrication and detection technique of PhHyd by microwires

AuE is fabricated with as-grown ZnO-Fe_2O_3 microwire using butyl carbitol acetate (BCA) and ethyl acetate (EA) as a conducting coating agent. Then it is placed into oven at 65.0 ^oC for 3 hours until the film is completely dry and uniform. 0.1 M phosphate buffer solution (PBS) at pH 7.0 is prepared by mixing 0.2 M Na_2HPO_4 and 0.2 M NaH_2PO_4 solution in 100.0 mL de-ionize water. A cell is consisted of ZnO-Fe_2O_3 microwire fabricated AuE as a working and Pd wire is used a counter electrodes. As received PhHyd is diluted to make various concentrations (1.0 nM ~ 1.0 M) in PBS solution and used as a target analyte. 10.0 mL of 0.1 M PBS solution is kept constant during measurements into the electrochemical cell. The ratio of current versus concentration (slope of calibration curve) is used to measure of target chemical sensitivity. Detection limit is measured from the ratio of $^{3N}/_{S}$ versus sensitivity (ratio of noise×3 vs. sensitivity) in the linear dynamic range of calibration plot. Electrometer is used as a voltage sources for I-V measurement in simple two electrodes system. The as-grown ZnO-Fe_2O_3 microwires are fabricated and employed for the detection of toxic PhHyd.

3. RESULTS AND DISCUSSION

3.1. Optical study

The optical property of the as-grown ZnO-Fe_2O_3 microwires is one of the significant characteristics for the assessment of its photo-catalytic activity. UV/visible absorption spectroscopy is

a technique in which the outer electrons of atoms or molecules absorb radiant energy and undergo transitions to high energy levels. In this phenomenon, the spectrum obtained due to optical absorption can be analyzed to acquire the energy band gap of the metal oxides. For UV/visible spectroscopy, the absorption spectrum of ZnO-Fe_2O_3 microwire solution is measured as a function of wavelength, which is presented in Figure 1A. It presents a broad absorption band around 302.0 nm in the visible-range between 200.0 to 800.0 nm wavelengths indicating the formation of ZnO-Fe_2O_3 microwires. Band-gap energy (E_{bg}) is calculated on the basis of the maximum absorption band of ZnO-Fe_2O_3 microwires and found to be 4.1059 eV, according to following equation (v).

$$E_{bg} = \frac{1240}{\lambda} \text{ (eV)} \qquad \text{(v)}$$

Where E_{bg} is the band-gap energy and λ_{max} is the wavelength (302.0 nm) of the ZnO-Fe_2O_3 microwires. No extra peak associated with impurities and structural defects were observed in the spectrums, which proved that the synthesized microstructure controlled crystallinity of as-grown ZnO-Fe_2O_3 microwires [39].

.

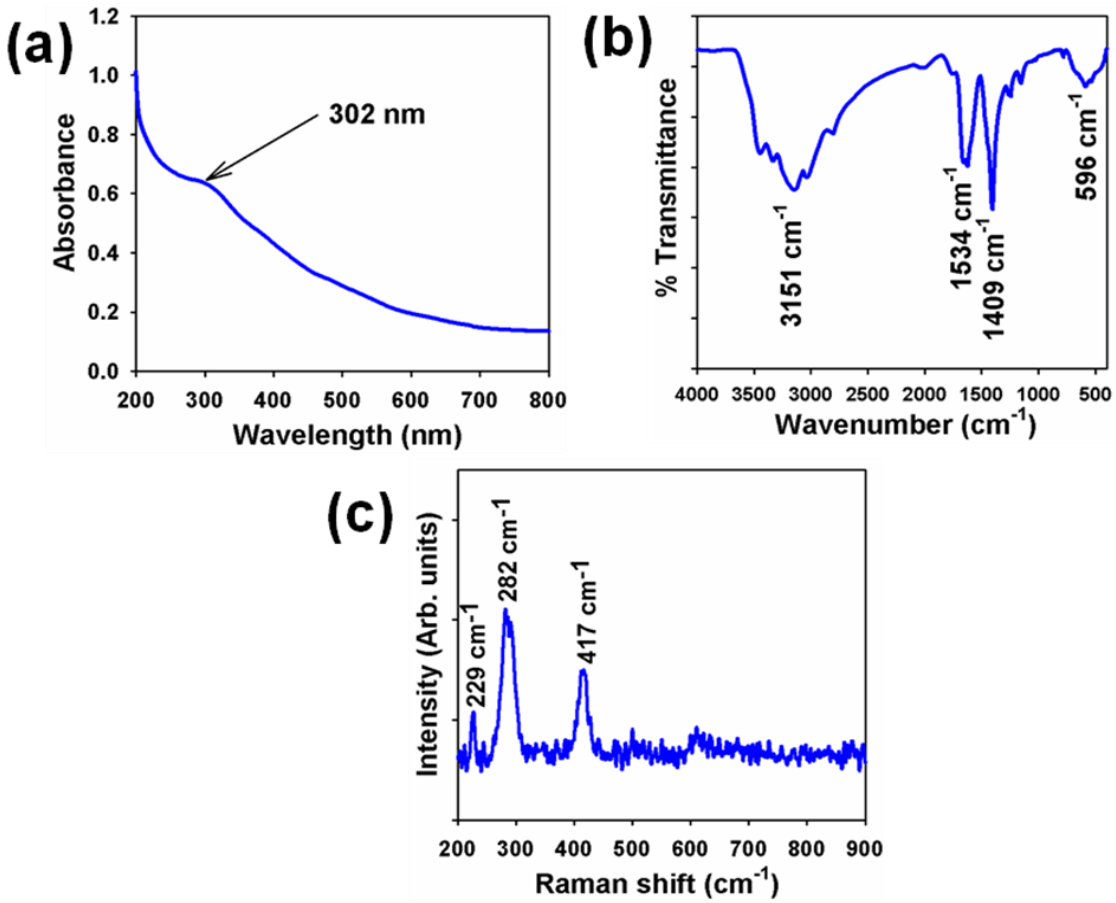

Figure 1. (a) UV/visible, (b) FT-IR, and (c) Raman spectroscopy of as-grown ZnO-Fe_2O_3 microwires at room conditions

The as-grown ZnO-Fe_2O_3 microwires are also studied in term of the atomic and molecular vibrations. To predict the functional-group identification, FT-IR spectra are investigated fundamentally in the region of 400 ~ 4000 cm^{-1} at room conditions. Figure 1B displays the FT-IR spectrum of the as-grown microwires. It represents band at 596, 1409, 1534, and 3151cm^{-1}. These observed broad vibration band (at 596 cm^{-1}) could be assigned as metal-oxygen (Fe-O and Zn-O mode) stretching vibrations, which demonstrated the configuration of ZnO-Fe_2O_3 microwires materials. The supplementary vibrational bands may be assigned to O-H bending vibration, C-O absorption, and O-H stretching. The absorption bands at 1409, 1534, and 3151 cm^{-1} generally shows from CO_2 and water, which usually semiconductor nanostructure materials absorbed from the environment due to their high surface-to-volume ratio of mesoporous nature [40]. Finally, the experimental vibration bands at low frequencies regions recommended the formation of ZnO-Fe_2O_3 microwires by a wet-chemical method.

Raman spectroscopy is a spectroscopic technique utilized to display vibrational, rotational, and other low-frequency phases in a Raman active compound. It depends on inelastic scattering of monochromatic light (Raman scattering), usually from a laser in the visible, near infra-red, or near ultra-violet range. The laser light relates with molecular vibrations, phonons or other excitation in the modes, showing in the energy of the laser photons being shifted up or down. The shift in energy represents the information regarding the phonon modes in the system, where infrared spectroscopy yields similar, but complementary information. Raman spectroscopy is generally established and utilized in material chemistry, since the information is specific to the chemical bonds and symmetry of metal-oxygen stretching or vibrational modes. Usually, there are three vibration modes in ZnO nanomaterial crystal: A_1, E_1 and E_2, of which A_1 and E_1 split into longitudinal (A_{1L}, E_{1L}) and transverse (A_{1T}, E_{1T}) ones and E_2 contains low and high frequency phonons (E_{2L} and E_{2H}) [41]. As-grown ZnO-Fe_2O_3 microwire is significantly altered the Raman spectra as well as the crystal of ZnO nanostructure [42]. Here, Figure 1c confirms the Raman spectrum, where key aspects of the wave number are executed at about 229 cm^{-1} and 282 cm^{-1} for metal-oxygen (Fe-O and Zn-O) stretching vibrations. The large bands can be assigned to a cubic phase of ZnO-Fe_2O_3 microwires. At 417 cm^{-1}, higher wave-number shift is revealed owing to the different dimensional effects of the microwires.

3.2. Morphological, Structural, and Elemental study

FE-SEM images of as-grown ZnO-Fe_2O_3 microwires structure are presented in Figure 2(a-b). It exhibits the images of the wire-shapes with micro-dimensional sizes of as-grown ZnO-Fe_2O_3 microwires. The dimension of microwire is calculated in the range of 13.89 μm. It is clearly exposed from the FE-SEM images that the facile synthesized ZnO-Fe_2O_3 is microwires in wire-shape, which is grown in very high-density and possessing almost uniform microwire shapes. When the size of doped material decreases into micrometer-sized scale, the surface area increases significantly, this improves the energy of the system, making re-distribution of Zn and Fe ions possible. The micrometer-sized wires could have tightly packed into the lattice, which is an agreement with the results obtained by scientist [43].

.

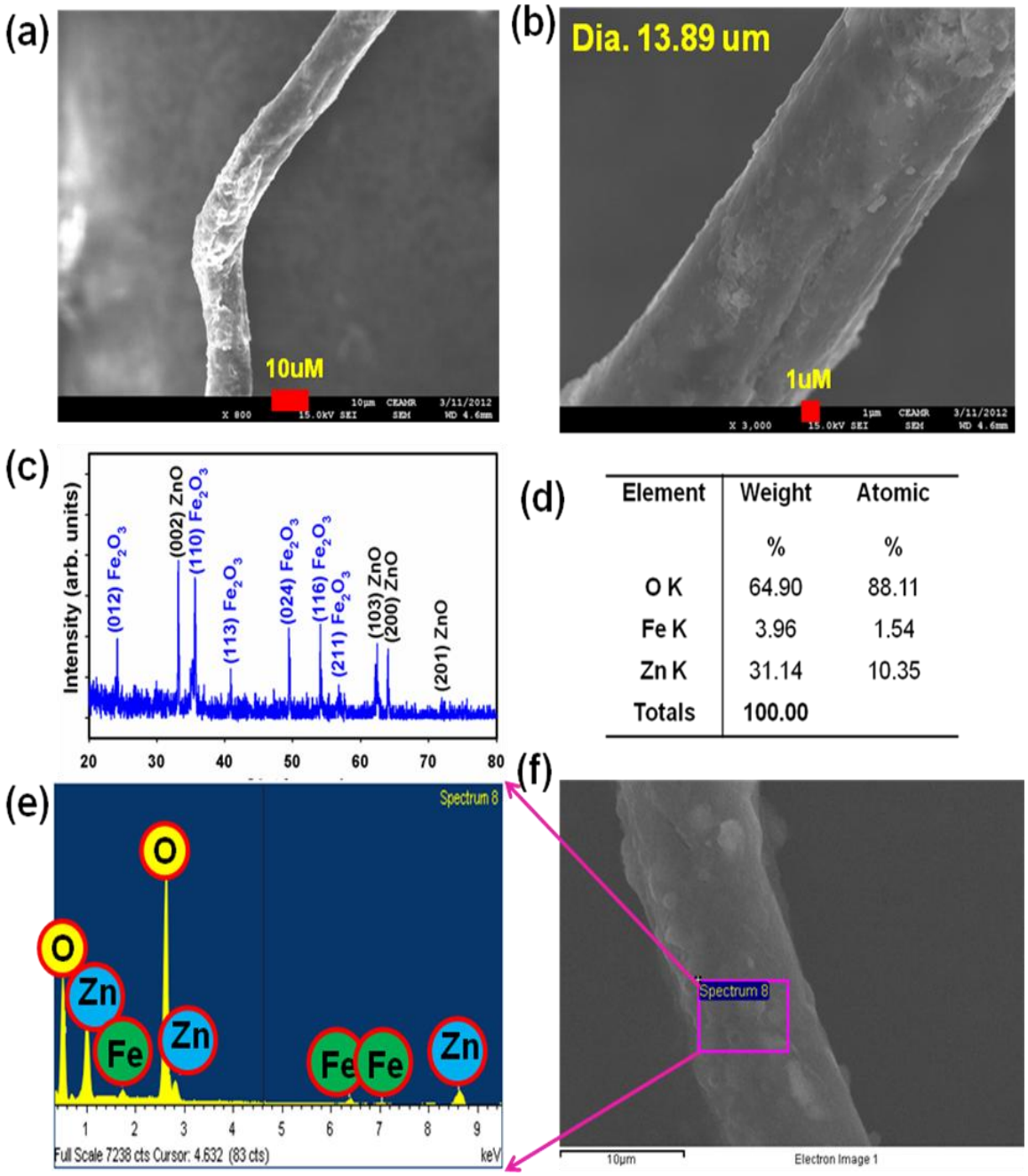

Figure 2. (a-b) FE-SEM images, (c) Powder x-ray diffraction pattern, and (d-f) Electron dispersive spectroscopy of as-grown ZnO-Fe_2O_3 microwires at room conditions.

Crystallinity and crystal phase of as-grown ZnO-Fe_2O_3 microwires were investigated in this study. X-ray diffraction patterns of codoped spinel microwires are represented in Figure 2c. The ZnO-Fe_2O_3 microwires samples were investigated and exhibited as face-centered cubic shapes. Figure 2c reveals the characteristic crystallinity of the ZnO-Fe_2O_3 microwires and their phase arrangement, which is investigated using powder X-ray crystallography. All the reflection peaks in this prototype were initiated to correspond with ZnO phase having face-centered cubic zincite geometry [JCPDS # 071-6424]. The phases are demonstrated the key features with indices for crystalline ZnO at 2θ values

of 33.5(002), 62.4(103), 63.9(200), and 72.1(201) degrees. The face-centered cubic lattice parameters are a= 3.2494, b=5.2038, and radiation ($CuK_\alpha1$, λ=1.5406). The ZnO phases have a high degree of crystallinity. All of the peaks match well with Bragg reflections of the standard zincite structure (point or space-group P63mc). The reflection peaks were also found to correspond with Fe_2O_3 phase having face-centered cubic hematite geometry [JCPDS # 089-0597]. The crystalline phases are demonstrated the key features with indices for crystalline Fe_2O_3 at 2θ values of 24.8(012), 35.7(110), 40.8(113), 49.5(024), 54.2(116), and 56.5(211) degrees. The face-centered cubic lattice parameters are a=5.039, c=13.77, Z=6 and radiation ($CuK_\alpha1$, λ=1.5406). The Fe_2O_3 phases have a high degree of crystallinity. All of the peaks are well matched with Bragg reflections of the standard hematite structure [point or space-group R-3c(167)]. It is confirmed that there is major number and amount of crystalline ZnO-Fe_2O_3 present in microwires [44]. The electron dispersive spectroscopy (EDS) investigation of as-grown ZnO-Fe_2O_3 microwires is indicated the presence of Zn, Fe, and O composition in the pure codoped material with adequate amount. It is clearly displayed that as-prepared codoped materials are well-controlled only with zinc, iron, and oxygen elements, which is presented in Figure 3d to Figure 3f. The composition of zinc, iron, and oxygen is 31.14%, 3.96%, and 64.90% respectively. No other peak related with any impurity has been detected in the EDS, which confirms that the microwires doped semiconductor products are composed only with zinc, iron, and oxygen.

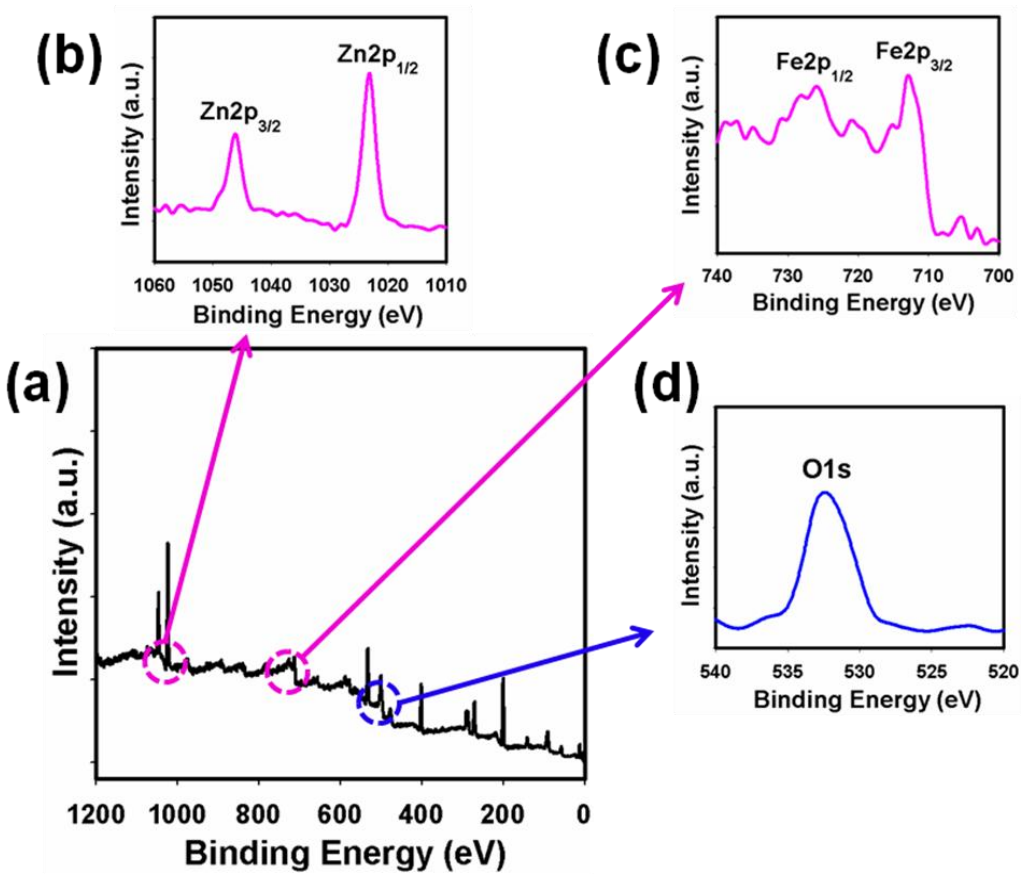

Figure 3. XPS of as-grown (a) ZnO-Fe_2O_3 microwires, (b) Zn2p level, (c) Fe2p, and (d) O1s level acquired with MgKα radiations.

X-ray photoelectron spectroscopy (XPS) is a quantitative spectroscopic method that determines the chemical-states of the elements that present within a doped materials. XPS spectra are acquired by

irradiating on a nanomaterial with a beam of X-rays, while simultaneously determining the kinetic energy and number of electrons that get-away from the top one to ten nm of the material being analyzed. Here, XPS measurements were measured for ZnO-Fe_2O_3 microwires semiconductor nanomaterials to investigate the chemical states of ZnO and Fe_2O_3. The XPS spectra of Zn2p, Fe2p, and O1s are presented in Fig. 3a. In Figure 3b, the spin orbit peaks of the $Zn2p_{(3/2)}$ and $Zn2p_{(1/2)}$ binding energy for all the samples appeared at around 1047 eV and 1022 eV respectively, which is in good agreement with the reference data for ZnO [45]. XPS was also used to resolve the chemical state of the doped Fe_2O_3 nanomaterial and their depth. Figure 3c presents the XPS spectra (spin orbit doublet peaks) of the $Fe2p_{(3/2)}$ and $Fe3p_{(1/2)}$ regions recorded with semiconductor codoped materials. The binding energy of the $Fe3p_{(3/2)}$ and $Fe3p_{(1/2)}$ peak at 713 eV and 725 eV respectively denotes the presence of Fe_2O_3 since their bindings energies are similar [46]. The O1s spectrum shows a main peak at 532 eV in Fig. 3d. The peak at 532 eV is assigned to lattice oxygen may be indicated to oxygen (ie, O_2^-) presence in the nanomaterials [47].

3.3. Detection of PhHyd using ZnO-Fe_2O_3 microwires

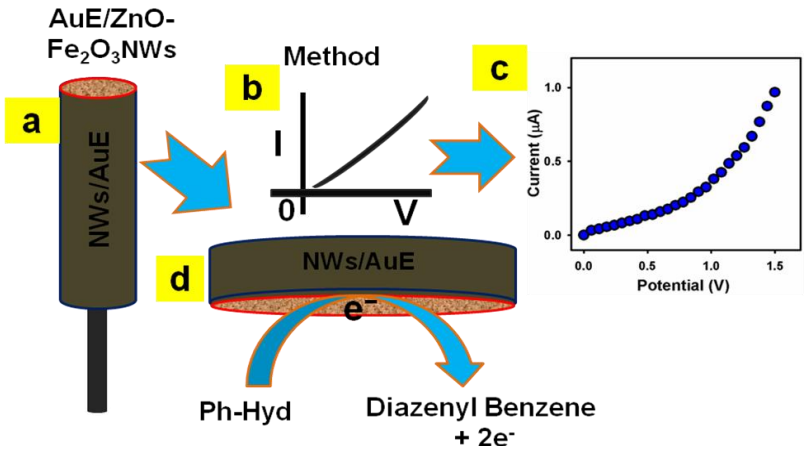

Figure 4. Schematic representation of (a) fabricated with microwires with conducting binders (EA and BCA), (b) I-V detection methodology (theoretical), (c) outcomes of I-V experimental result, and (d) reaction mechanism of PhHyd in presence of codoped ZnO-Fe_2O_3 microwires.

The potential application of as-grown ZnO-Fe_2O_3 microwires for chemical sensors has been used for measuring and detecting toxic chemicals, which are not environmental affable. The microwires modified chemi-sensors have advantages such as stable in air, non-toxicity, electrochemical activity, and easy to assemble [48,49]. As in the case of PhHyd sensors, the main purpose was to measure the current response using simple I-V method with ZnO-Fe_2O_3 microwires. The fabricated-surface of codoped sensor is made with binders on the AuE (Figure 4a). The fabricated AuE was put into oven at 65.0 ^oC for 12 hr to make it dry and uniform. Theoretical I-V signals of sensor are proposed having codoped film as a function of current versus potential (Figure 4b). The responses of analyte are employed by reliable I-V technique ZnO-Fe_2O_3 microwires fabricated AuE film (Figure 4c). The probable reaction mechanism is generalized in presence of analyte on ZnO-Fe_2O_3

microwires surfaces by I-V method (Figure 4d). Here, PhHyd is converted to diazenyl benzene in presence of doped ZnO-Fe_2O_3 microwires by releasing electrons ($2e^-$) to the reaction system, which improved and enhanced the current responses against potential during the I-V process at room conditions.

Figure 5a displays the current responses without (gray-dotted) and with (dark-dotted) coating of ZnO-Fe_2O_3 microwires on AuE surfaces. With microwires fabricated surface, the current signal is reduced compared to without fabricated surface, which indicated the surface is slightly blocked with codoped materials. The current changes are plotted for the microwires modified film before (gray-dotted) and after (blue-dotted) injecting of 50.0 µL PhHyd in 10.0 mL PBS (Figure 5b). The surface current is investigated in every injection of analyte into the solution. 10.0 mL of 0.1M PBS solution is put into the cell and added the low to high concentration of target drop-wise from the stock solution. The current responses with ZnO-Fe_2O_3 microwires modified AuE are measured from the various concentrations (1.0 nM to 1.0 M) of PhHyd (Figure 5c). It shows the current changes are observed with fabricated AuE as a function of analyte concentration at room conditions. It is also observed that at low to high concentration of analyte, the current response is enhanced slowly. A calibration curve is plotted in higher potential range (calibration curve) based on analyte concentrations (Figure 5d). A large range of PhHyd concentration is selected to examine the probable analytical parameters, which is used in 1.0 nM to 1.0 M. The sensitivity is calculated from the calibration curve, which is close to 8.33 $\mu Acm^{-2}mM^{-1}$. The linear dynamic range of PhHyd sensor displays from 1.0 nM to 10.0 mM (r^2 = 0.9389) and the detection limit was considered as 0.67 nM [3×noise (N)/slope(S)].

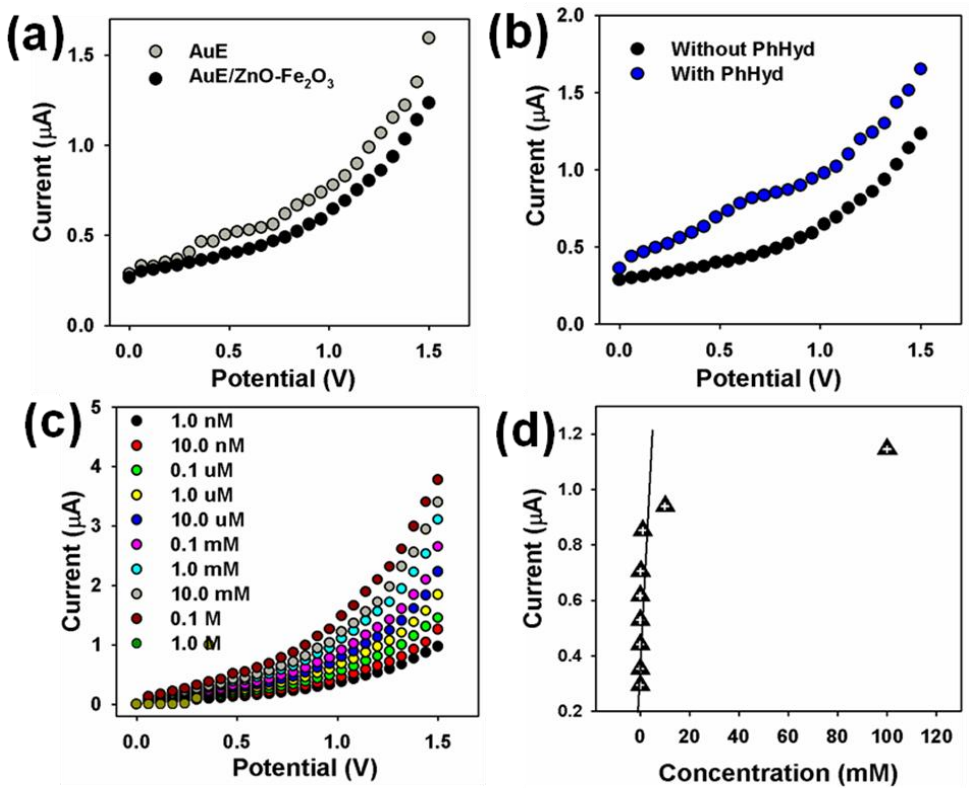

Figure 5. I-V responses of (a) without and with coating; (b) without and with PhHyd; (C) concentration variations; and (d) calibration plot of ZnO-Fe_2O_3 microwires fabricated on AuE.

During the detection of analyte with fabricated AuE, the resistance values of sensors are decreased with increasing working condition due to the fundamental characteristics of the semiconductor codoped materials [50]. Here, oxygen adsorption exhibits an essential responsibility in the electrical properties of the ZnO-Fe_2O_3 material with microwires structures [Figure 6a]. Adsorbed oxygen ion eliminates the conduction electrons and enhances the resistance of AuE. Reactive oxygen species (i.e., O_2^- and O^-) are adsorbed on the ZnO-Fe_2O_3 surface, where the amount of such chemisorbed oxygen species strongly depends on the structural properties of codoped microwires. At room conditions, O_2^- is chemisorbed, while in microwires morphology, O_2^- and O^- are chemisorbed, and the O_2^- disappears quickly [51]. Here, PhHyd sensing mechanism of ZnO-Fe_2O_3 sensor is also based on the semiconductors metal oxides, due to the oxidation or reduction of the microwires, according to the dissolved O_2 in bulk-solution or surface-air of the adjacent atmosphere [Figure 6b], according to the equations (vi-vii).

$$e^- (ZnO\text{-}Fe_2O_3) + O_2 \rightarrow O_2^- \qquad \text{(vi)}$$

$$e^- (ZnO\text{-}Fe_2O_3) + O_2^- \rightarrow 2O^- \qquad \text{(vii)}$$

These reactions are attained in bulk-system or air/liquid interface or surrounding air due to the small carrier concentration which enhanced the resistance. The PhHyd sensitivity towards ZnO-Fe_2O_3 could be accredited to high oxygen shortages, which amplify the oxygen adsorption. Larger the amount of oxygen adsorbed on the sensor surface, higher would be the oxidizing potentiality and faster would be the oxidation of PhHyd.

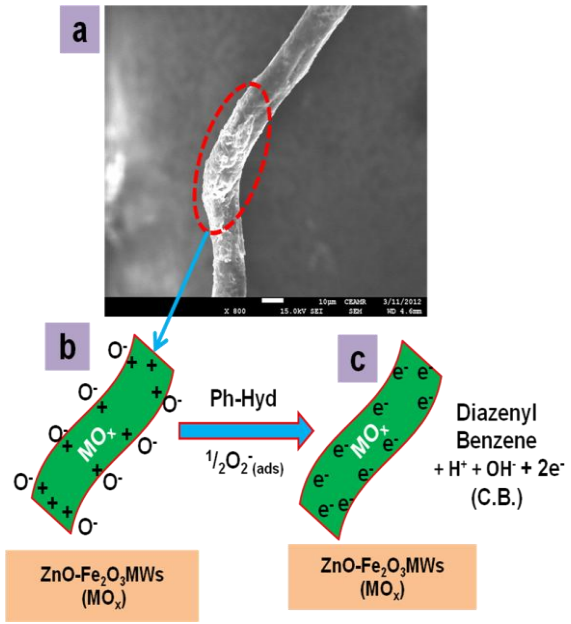

Figure 6. Mechanism of calcined ZnO-Fe_2O_3 microwires phenyl hydrazine sensors at ambient conditions. (a) Magnified FE-SEM image of doped nanomaterials, (b) Reactive oxygen species are adsorbed on doped surface, and (c) PhHyd reacts with the adsorbed oxygen on doped surface.

The reactivity of PhHyd would have been very large as contrasted to other chemical with the surface under same situation [52]. When PhHyd reacts with the adsorbed oxygen ($^1/_2O_2^-$) on the exterior/interior of the layer, it oxidized to diazenyl benzene and metal PhHyd, liberating free electrons ($2e^-$) in the conduction band could be uttered through the following reactions [equation (viii) to (x)], which is presented in Figure 5c.

$$PhHyd + {}^1/_2O_2^- \rightarrow \text{Diazenyl Benzene} + H^+ + OH^- + 2e^- \text{ (C.B.)} \quad \text{(viii)}$$

$$H^+ + OH^- \rightarrow H_2O \quad \text{(ix)}$$

$$\text{Diazenyl Benzene} + {}^1/_2O_2 + H^+ \rightarrow \text{Benzenediazonium} + H_2O \quad \text{(x)}$$

These reactions corresponded to oxidation of the reducing carriers. These methods increased the carrier concentration and hence decreased the resistance on revelation to reducing PhHyd analyte. At the room conditions, the exposure of doped surface towards the reducing agents is resulted in a surface mediated incineration process. The elimination of iono-sorbed oxygen increases the electron concentration, which enhances the surface conductance of the fabricated AuE film [53]. The reducing PhHyd analyte donates electrons to ZnO-Fe_2O_3 fabricated AuE surface. Hence, the resistance is decreased and conductance is increased. This is the key factor of analyte response (current response) enhancement with increasing potential. Thus generated electrons contribute to sudden increase in conductance of the fabricated film. The ZnO-Fe_2O_3 unusual regions dispersed on the surface would increase the ability of microwires to absorb more oxygen species giving high resistance in air ambient. The response time was approximately 10.0 sec for the ZnO-Fe_2O_3 fabricated AuE to achieve saturated steady state current. The elevated sensitivity of sensor can be attributed to the good absorption (permeable surfaces fabricated with binders), adsorption capability (microstructure materials), high catalytic properties, and good biocompatibility of the ZnO-Fe_2O_3 microwires. The efficient sensitivity of the fabricated sensor is comparatively superior to formerly reported chemi-sensors based on other composite or materials modified electrodes [54-57]. Due to large surface area of fabricated-AuE, the doped-materials offered a constructive microenvironment for the chemical recognition with efficient number. The higher sensitivity of ZnO-Fe_2O_3 microwires afforded high electron communication features which improved the direct electron-communication between the active sites of microwires and AuE-electrodes. In Table 1, it is compared the performances for phenyl hydrazine chemical detection based ZnO-Fe_2O_3 microwires using various modified electrode materials [58-62]. The modified doped-film had a superior stability. Moreover, due to high active surface area, the microwires conveyed constructive surroundings for the PhHyd detection (by adsorption) in huge-amount. The ZnO-Fe_2O_3 microwires display several approaching in providing chemical based sensors and encouraging improvement has been accomplished in the research fragment. As for the microwires, doped semiconductor materials offer a route to a novel production of chemi-sensors and a premeditate attempt has to be forwarded for codoped microstructures to be taken considerably for large extent applications. The PhHyd chemical sensor based on microwires is displayed good reproducibility and stability for over two weeks and no major changes in sensor responses are found. After two weeks, the

chemi-sensor response with codoped microwires is slowly decreased, which may be due to the weak-interaction between fabricated microwires active surfaces and PhHyd chemical. The significant result is achieved by wet-chemical process to prepare ZnO-Fe_2O_3 microwires, which can be employed as efficient electron mediators for the development of effective chemical sensors.

Table 1. Comparison the performances for phenyl hydrazine detection based various material fabricated electrodes.

Materials	Methods	Full conc. Range	LDR	Linearity (r^2)	Sensitivity	DL	Ref.
Carbon Nanotube Paste Electrode	Cyclic Voltammetry	6.0×10^{-7} M~ 9.0×10^{-4} M	0.6 ~900.0 µM	0.9991	--	1.31×10^{-7} M	[58]
Carbon paste electrode	Cyclic Voltammetry	0.025 ~ 0.2 mM	0.025 ~ to 0.1 mM	0.9970	--	2.5 µM	[59]
Glassy carbon electrode	Amperometric method	--	2.0~20.0 µM	--	0.016 $\mu A\mu M^{-1}$	0.05 µM	[60]
Carbon paste electrode	Amperometric method	1.0~70.0 mM	0.1~6.0 mM	0.9984	--	40.0 µM	[51]
Carbon Paste Electrode	Cyclic Voltammetry	0.07~900 µM	7.0×10^{-8} ~ 9.0×10^{-4} M	--	0.016 $\mu A.\mu M^{-1}$	40.0 nM	[62]
ZnO-Fe_2O_3 MWs/AuE	I-V method	1.0 nM ~ 1.0 M	1.0 nM ~ 10.0 mM	0.9389	8.33 $\mu Acm^{-2}mM^{-1}$	0.67 ± 0.05 nM	Current report

4. CONCLUSION

Due to numerous potential applications of transition metal-doped semiconductor materials, a well-crystalline as-grown ZnO-Fe_2O_3 microwire is prepared by simple wet-chemical process at low temperature. The detailed structural, morphological and optical characterizations are confirmed that the synthesized microwires are well-crystalline with face-centered cubic and possessing good optical properties. Microwires are exhibited higher-sensitivity and lower-detection limit with good linearity in short response time, which is efficiently utilized as chemi-sensor for the fabrication of PhHyd. This novel attempt was to introduce a well-organized route of efficient toxic chemi-sensor development for environmental hazardous pollutants and health-care fields in large scale.

ACKNOWLEDGMENTS

This paper was funded by King Abdulaziz University, under grant No. (31-3-1432/HiCi). The authors, therefore, acknowledge technical and financial support of KAU.

References

1. A. Kumar, A. Singhal. *Nanotechnology* 18 (2007) 475703-475710.
2. M.M. Rahman, S.B. Khan, M. Faisal, A.M. Asiri, K.A. Alamry, *Sens. Actuator B: Chem*. 171-172 (2012) 932-937.

3. M.M. Rahman, S.B. Khan, M. Faisal. A.M. Asiri, M. A. Tariq, *Electrochim. Acta* 75 (2012) 164-170.
4. M.M. Rahman, A. Jamal, S.B. Khan, M. Faisal. A.M. Asiri, *Microchim. Acta* 178 (2012) 99-106.
5. M.M. Rahman, A. Jamal, S.B. Khan, M. Faisal. A.M. Asiri, Talanta 95 (2012) 18-24.
6. M.M. Rahman, A. Jamal, S.B. Khan, M. Faisal. A.M. Asiri, *Chem. Engineer. J.* 192 (2012) 122-128.
7. M.M. Rahman. *J. Biomed. Nanotech.* 7 (2011) 351-357.
8. M.M. Rahman. *Sens. Transduc. J.* 126 (2011) 11-18.
9. M.M. Rahman. *Natur. Sci.* 3 (2011) 208-217.
10. M.M. Rahman. *Inter. J. Biolog. Med. Res.* 1 (2010) 9-14.
11. M.M. Rahman. *J. Mater. Sci. Engineer.* 4 (2010) 39-49.
12. M.M. Rahman, A. Umar, K. Sawada. *Advan. Sci. Lett.* 2 (2009) 28-34.
13. G.M. Whitesides, M. Boncheva. *Proc. Natl. Acad. Sci. USA*. 99 (2002) 4769-4774.
14. L. Dale, Huber. *Small* 1 (2009) 482-501.
15. N.M. Shaalan, T. Yamazaki, T. Kikuta. *Sens. Actuator. B* 153 (2011) 11-16.
16. A. Umar, M.M. Rahman, S.H. Kim, Y.B. Hahn. *Chem. Commun*. (2008) 166-169.
17. C. Yao, Q. Zeng, G.F. Goya, T. Torres, J. Liu, H. Wu, M. Ge, Y. Zeng, Y. Wang, J.Z. Jiang, *J. Phys. Chem. C*. 111 (2007) 12274–12278.
18. W.B. Ingler-Jr, J.P. Baltrus, S.U.M. Khan, *J. Am. Chem. Soc*. 126 (2004) 10238-10239.
19. S.B. Khan, M.M. Rahman, K. Akhtar, A.M. Asiri, J. Seo, H. Han, K. Alamry. *Int. J. Electrochem. Sci*.7 (2012) 4030-4038.
20. M. Grigorova, H.J. Blythe, V. Blaskov, V. Rusanov, V. Petkov, V. Masheva, D. Nihtianova, L.M. Martinez, J.S. Munoz, M. Mikhov, *Magn. Magn. Mater*. 183 (1998) 163-168.
21. C.H. Yang, H.J. Lee, Y.B. Kim, S.J. Han, Y.H. Jeong, N.O. Birge, *Physica B*. 383 (2006) 28–30.
22. F. Grasset, N. Labhsetwar, D. Li, *Langmuir.* 18 (2002) 8209–8216.
23. H. Deng, X. Li, Q. Peng, X. Wang, J. Chen, Y. Li, *Angewandte Chemie. (Inter. Ed.)*. 44 (2005) 2782–2785.
24. J.A. Toledo-Antonio, N. Nava, M. Martınez, X. Bokhimi, *App. Cat. A*. 234 (2002) 137–144.
25. J. Fu, D. Gao, Y. Xu, Z. Yan, D. Xue, *Chem. Mat*. 20 (2008) 2016–2019.
26. G. Zhang, C. Li, F. Cheng, J. Chen, *Sens. Actuator B*. 120 (2007) 403-410.
27. B. Kazinczy, L. Kótai, I Gács, I.E. Sajó, B. Sreedhar, K. Lázár, *Ind. Eng. Chem. Res*. 42 (2003) 318–322.
28. S.R. Lee, M.M. Rahman, M. Ishida, K. Sawada, *Trends in Anal. Chem*. 28 (2009) 196-199.
29. M.M. Rahman, S.B. Khan, H.M. Marwani, A.M. Asiri, K.A. Alamry, A.O. Al-Youbi. *Talanta* 104 (2013) 75-82.
30. M.M. Rahman. *J. Mater. Sci. Engineer. B.* 2 (2012) 30-39.
31. M.M. Rahman, A. Jamal, S.B. Khan, M. Faisal. A.M. Asiri. *Sens. Transduc. J.* 134 (2011) 32-44.
32. M.M. Rahman, A. Jamal, S.B. Khan, M. Faisal. *J. Phys. Chem. C* 115 (2011) 9503–9510.
33. M.M. Rahman, A. Jamal, S.B. Khan, M. Faisal. *Biosens. Bioelectron.* 28 (2011) 127-134.
34. M.M. Rahman, A. Jamal, S.B. Khan, M. Faisal. *Superlatt. Microstruc.* 50 (2011) 369-376.
35. M.M. Rahman, A. Jamal, S.B. Khan, M. Faisal. *ACS App. Mater. Inter.* 3 (2011) 1346-1351.
36. M.M. Rahman, I.C. Jeon. *J. Braz. Chem. Soc.* 18 (2007) 1150-1157
37. M.M. Rahman, I.C. Jeon. *J. Organomet. Chem.* 691 (2006) 5648-5654.
38. J.D.A. Gomes, M.H. Sousa, F.A. Tourinho, R. Aquino, G.J.D. Silva, J. Depeyrot, E. Dubois, R. Perzynski, *J. Phys. Chem. C*. 112 (2008) 6220-6227.
39. M.M. Rahman, A. Umar, K. Sawada, *Sens. Actuator B*. 137 (2009) 327-332.
40. W. Jiang, Z. Cao, R. Gu, X. Ye, C. Jiang, X. Gong, *Smart. Mater. Struct*. 18 (2009) 125013-12016.
41. N. Han, L. Chai, Q. Wang, Y. Tian, P. Deng, Y. Chen, *Sens. Actuator. B*. 147 (2010) 525-530.
42. Y. Li, R. Yi, A. Yan, L. Deng, K. Zhou, X. Liu, *Sol. Stat. Sci*. 11 (2009) 1319-1324.
43. T.C. Damen, S.P.S. Porto, B. Tell, *Phys. Rev*. 142 (1966) 570-574.

44. C. Bundesmann, N. Ashkenov, M. Schubert, D. Spemann, T. Butz, E.M. Kaidashev, M. Lorenz, M. Grundmann, *Appl. Phys. Lett*. 83 (2003) 1974-1976.
45. M.M. Rahman, A. Jamal, S.B. Khan, M. Faisal, *J. Nanopart. Res*. 13 (2011) 3789–3799.
46. R.F. Mulligan, A.A. Iliadis, P. Kofinas, *J. App. Poly. Sci*. 89 (2003) 1058-1061.
47. T. Fujii, F.M.F. de Groot, G.A. Sawatzky. F.C. Voogt, T. Hibma, K. Okada. *Physical Review B.* 59 (1999) 3195-3202.
48. M.M. Rahman, S.B. Khan, M. Faisal, M.A. Rub, A.O. Al-Youbi, A.M. Asiri. *Talanta* 99 (2012) 924-931.
49. C. Yao, Q. Zeng, G.F. Goya, T. Torres, J. Liu, H. Wu, M. Ge, Y. Zeng, Y. Wang, J.Z. Jiang, *J. Phys. Chem. C* 111 (2007) 12274-12278.
50. L. Zhuo, Y. Huang, M.S. Cheng, H.K. Lee, C.S. Toh, *Anal. Chem*. 82 (2010) 4329-4332.
51. A. Hierlemann, R. Gutierrez-Osuna, *Chem. Rev.* 108 (2008) 563-613.
52. P. Song, H.W. Qin, L. Zhang, K. An, Z.J. Lin, J.F. Hu, M.H. Jiang, *Sens. Actuators B: Chem.* 104 (2005) 312-316.
53. T.J. Hsueh, C.L. Hsu, S.J. Chang, I.C. Chen, *Sens. Actuator. B. Chem.* 126 (2007) 473-477.
54. D.R. Patil, L.A. Patil, P.P. Amalnerkar, *Bull. Mat. Sci*. 30 (2007) 553-559.
55. S. Mujumdar, *Mat. Sci. Poland*. 27 (2009) 123-129.
56. V.B. Raj, A.T. Nimal, Y. Parmar, M.U. Sharma, K. Sreenivas, V. Gupta, *Sens. Actuator. B* 147 (2010) 517-524.
57. K. Raj, B. Moskowitz, R. Casciari, *J. Magn. Magn. Mater.* 149 (1995) 174-180.
58. N. Rastakhiz, A.Kariminik, V. Soltani-Nejad, S. Roodsaz, *Int. J. Electrochem. Sci*. 5 (2010) 1203.
59. S. Chitravathi, B.E.K Swamy, U. Chandra, G.P. Mamatha, B.S. Sherigara, *J. Electroanal. Chem*. 645 (2010) 10-15.
60. H.M. Nassef, A. Radi, C.K. O'Sullivan, *J. Electroanal. Chem*. 592 (2006) 139-146.
61. R.E. Sabzi, E. Minaie, K. Farhadi, M.M. Golzan, *Turk. J. Chem*. 34 (2010) 901.
62. M.R. Akhgar, M.S.H. Zamani, A. Changizi, H. Hosseini-Mahdiabad, *Int. J. Electrochem. Sci*. 5(2010) 782.